Fourier Transform Infrared Investigation of the Deformation Behavior of Montmorillonite in Nylon-6/Nanoclay Nanocomposite

Leslie S. Loo and Karen K. Gleason*

Department of Chemical Engineering, Massachusetts Institute of Technology, Cambridge, Massachusetts 02139

Received December 3, 2002

Revised Manuscript Received February 14, 2003

Introduction. Recent interest in polymer/nanoclay nanocomposite systems is motivated by the possibility of achieving enhanced properties and added functionality at lower clay loading as compared to conventional micron size fillers. For instance, adding montmorillonite clay to nylon-6 increases modulus, yield strength, and heat distortion temperature[1] and also improves barrier[2] and ablative[3] properties. Since only a small amount of the inorganic material is needed to produce these desired characteristics, the nanocomposites can often be easily processed using existing methods. There is the potential for this new class of polymer systems to replace composite materials in the future. Consequently, it is important to understand the role of nanoclay in enhancing mechanical behavior. Since the thickness of one clay platelet is on the order of 1 nm, it is crucial to formulate experiments and models that can provide insight into the deformation process at the molecular level.

The structure of polymer nanocomposites has been examined by wide-angle X-ray scattering (WAXS), small-angle X-ray scattering (SAXS), transmission electron microscopy (TEM),[4] Fourier transform infrared spectroscopy (FTIR),[5] and nuclear magnetic resonance (NMR).[6] Various authors have also investigated their mechanical properties as a function of processing conditions, degree of exfoliation of nanoclay, and type of surfactant.[7,8] However, there are very few reports that directly probed the deformation of nanoclay particles in the polymer matrix.[9] In the past, WAXS has been used to monitor the strain in crystalline materials through stress-induced peak shifts.[10] However, if the nanoclay is exfoliated in the polymer, X-ray techniques cannot pick up any clay peaks. Consequently, spectroscopic techniques such as FTIR offer a very good way to observe deformation in nanoclay from stress-induced peak shifts. Such peak shifts in FTIR have first been studied by Zhurkov and co-workers to find out how the applied mechanical stress imposed upon a polymer sample is distributed among the interatomic bonds.[11−13] Later investigators utilized FTIR and Raman peak shifts to gain an understanding of the molecular mechanism of deformation in highly drawn homopolymers.[14] Raman spectroscopy has been particularly useful in the study of micromechanics of polymer fibers and composites.[15−17] An excellent review article has been written by Andrews et al.[18] Recently, Cooper and Young extended the capability of the Raman technique to studying reinforcement by nanoparticles, their system of interest being carbon nanotubes in an epoxy resin.[19] To the authors' knowledge, this is the first time that the deformation of nanoclay particles in a polymeric system has been studied by FTIR.

Materials and Methods. Pellets of grade 1022B homopolymer nylon-6 and grade 1022C5 nylon-6 containing 5 wt % montmorillonite clay (NY6NC) were obtained from UBE Industries. The mean molecular weight of the polymer (in both the homopolymer and nanocomposite samples) quoted by the manufacturer was approximately 22 000 g/mol. The nanocomposite was made by in situ polymerization.[20] The pellets were dried in a vacuum oven for more than 24 h at room temperature and then stored in a desiccator. To produce thin films suitable for FTIR measurements, the pellets were dissolved in 2,2,2-trifluoroethanol (0.50−0.70 g of pellets in 10 mL of solvent), and the solution was spun-cast onto a Teflon substrate with a flat surface. The solvent was then removed by heating the film and substrate in a vacuum between 75 and 80 °C for more than 12 h and cooled to room temperature. The resulting film was peeled off the substrate and cut to nominal gage length of 10 mm and width of 10 mm. The homopolymer film that was formed in this manner contained mostly α crystals. It was converted to primarily γ form by standard iodine treatment.[21] Finally, the films were dried at room temperature in a vacuum oven for at least 24 h and stored in a desiccator prior to use.

A Nicolet Nexus 870 FTIR spectrometer equipped with a commercial stretching device (Manning Applied Technology) was used to perform the deformation experiments. The detector is mercury cadmium telluride (MCT-A) with a range of 650−4000 cm^{-1}. The resolution is 4 cm^{-1}. The thickness of the films, measured with a digital micrometer at the end of the experiment (in order to prevent creasing), was between 5 and 6 μm. The film was held between two jaws, and 10 spectra of 64 scans each were taken of the unstretched film. The average position of each peak and the corresponding standard deviation were then determined. One of the jaws was fixed in position, and the film was manually stretched in increments of 0.05 mm by means of a micrometer attached to the other jaw. After stretching the film to a new position, a 5 min relaxation period was allowed for purging in order to obtain better signal-to-noise ratio before a spectrum (64 scans) was collected. Each spectrum was zero-filled twice, and the peak picking routine in the Omnic version 6 software was used to locate the position of each peak. Four sets of experiments were performed at room temperature to ensure reproducibility.

Results and Discussion. All the nanocomposite films were found to be brittle and tore completely into two pieces at low strains (defined as the change in the length of the sample divided by the original length) of less than 5%. The solid curve in Figure 1a shows the spectrum of NY6NC in the region containing the peak of the Si−O stretching vibration at about 1020 cm^{-1}.[22] The peak has more than one component. The dashed curve shows the spectrum at 2% strain. The Si−O stretching peak has clearly shifted to lower wavenumbers at the higher strain. In the FTIR spectrum of the torn film, the Si−O stretching peak was observed to shift back to its original position. This indicates that the peak shift is due to the imposed stress (or strain) on the specimen.

Even though the FTIR spectra of nylon-6 containing montmorillonite clay have been studied before,[23] no

10.1021/ma0259057 CCC: $25.00
Published on Web 03/19/2003

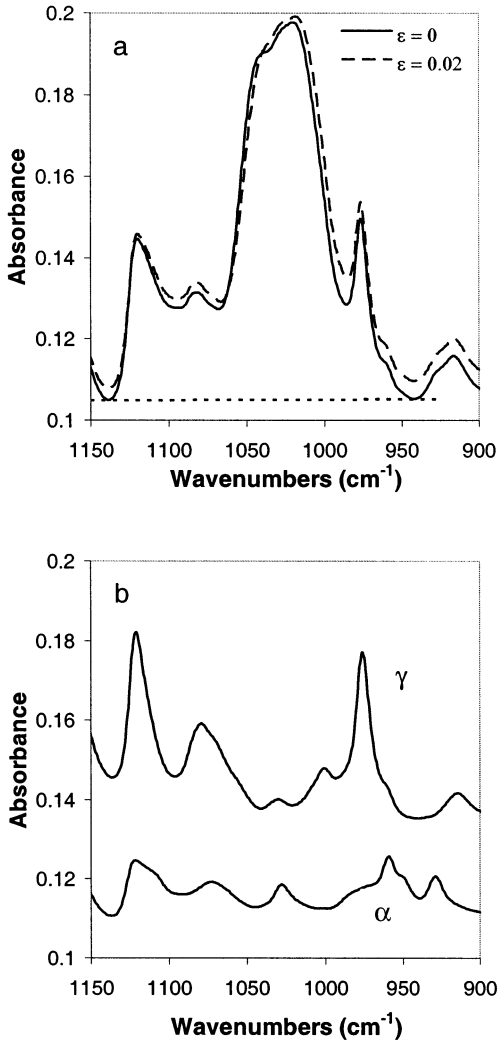

Figure 1. FTIR spectra of (a) NY6NC showing Si−O stretching region at 0 strain (solid line) and 0.02 strain (dashed line) and (b) nylon-6 with predominantly γ phase (top) and α phase (bottom). The dotted line in (a) shows the baseline used for baseline correction.

attempts were made to identify the individual Si−O stretching modes which have been observed in pure clay.[22] Figure 1b shows the FTIR spectra of nylon-6 containing primarily α and γ crystal phases, respectively. The presence of γ crystals in NY6NC is evidenced by the dominant peaks at 1122 and 976 cm^{-1}. The presence of a weak shoulder at 929 cm^{-1} and a strong amide II vibration at 1548 cm^{-1} (not shown) indicate that there are also some α crystals present in the nanocomposite. It has been postulated that the clay particles facilitate preferential formation of the γ crystals near the clay surface.[4]

Figure 2 shows the nonlinear least-squares regression of the spectrum in the Si−O stretching region. The spectrum was baseline corrected (see dotted line in Figure 1a) and fitted with 11 symmetric Gaussian peaks based on known assignments of nylon-6[21] and clay[22] peaks allowing only the peak position, peak height, and peak fwhm (full width at half-maximum) to vary. Figure 2 shows the 11 peaks used to fit the spectrum, and their assignments are as follows: 1122 cm^{-1} (C−C stretch), 1115 cm^{-1} (C−C stretch), 1100 cm^{-1} (Si−O stretch of clay), 1082 cm^{-1} (Si−O stretch of clay and CONH of nylon-6), 1046 cm^{-1} (Si−O stretch of clay), 1030 cm^{-1} (CONH), 1018 cm^{-1} (Si−O stretch of clay), 976 cm^{-1}

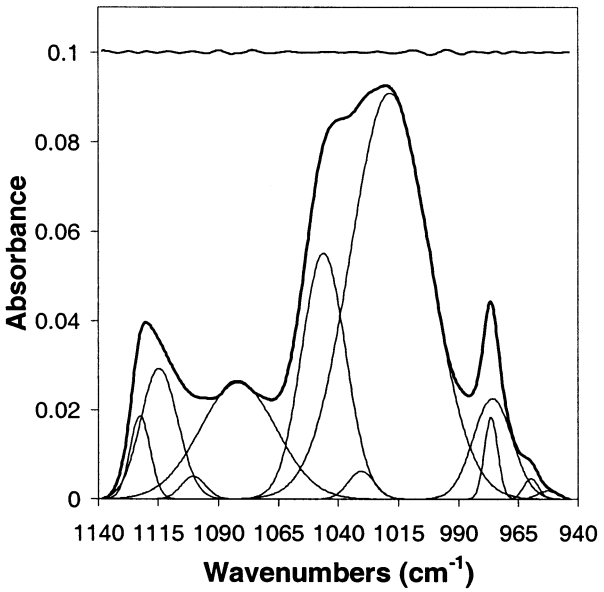

Figure 2. Nonlinear least-squares regression of the Si−O stretching region. The curve above the spectrum shows the difference between the best fit and actual data.

(CONH of γ crystal), 976 cm^{-1} (CONH of mesomorphous nylon-6), 960 cm^{-1} (CONH of α crystal), 953 cm^{-1} (CONH of α crystal). The exact assignments for some of these nylon-6 peaks are still debated in the literature. The weak Si−O stretching peak at 1100 cm^{-1} represents the in-plane (parallel) vibrations b_2^1 and b_2^3 (or a linear combination of these) while the one at 1082 cm^{-1} represents the out-of-plane (perpendicular) vibration mode a_1^1. The two strong peaks at 1046 and 1018 cm^{-1} also represents in-plane vibration modes b_1^1 and b_2^2, respectively.[22] The 1018 and 1046 cm^{-1} peaks in the nanocomposite spectrum (Figure 1a) can be attributed solely to the Si−O vibrations since there are no contributions from nylon-6 in this region. Furthermore, the only nylon-6 peak at about 1030 cm^{-1} has a much smaller intensity compared to the clay peaks. The other two clay peaks at 1100 and 1082 cm^{-1} have more overlap with nylon-6 peaks. Consequently, we shall consider the peak shift data only from the 1018 and 1046 cm^{-1} vibrations to be more meaningful.

Figure 3 shows the graph of peak shift (relative to the position at zero strain) vs strain for the 1022 cm^{-1} peak in the original spectrum and the individual fitted peaks at 1018 and 1046 cm^{-1}. A monotonic negative shift is observed for the peaks. The small magnitude of the standard deviation compared to that of the frequency shift indicates that this is a good method to monitor the stress on the clay particles. The 1018 cm^{-1} peak appears to show a slightly greater amount of shift compared to the 1046 cm^{-1} peak. The positions of all three peaks reverted back to the frequency at zero strain upon brittle fracture. This shows that the deformation of the clay particles is fairly elastic. Peak shifts in clay have been observed before as a result of water molecules penetrating between individual clay layers. The 1046 and 1018 cm^{-1} peaks shifted by as much as 5 and 15 cm^{-1}, respectively, in sodium montmorillonite.[24] This phenomenon has been attributed to changes in the Si−O structure of clay. In our system the only perturbation was due to imposed stress; hence, the frequency shift must therefore be due to changes in structure arising from the deformation of the clay platelets. Examples are

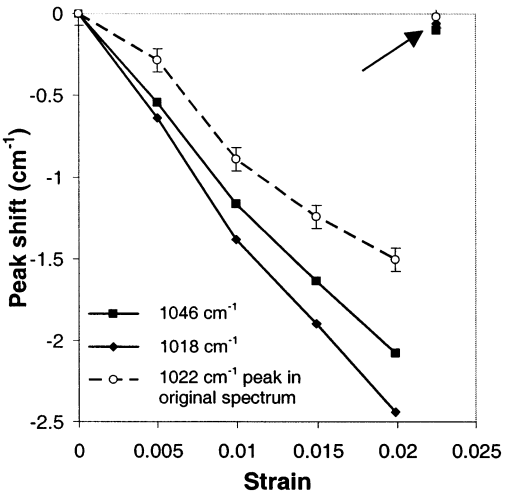

Figure 3. Graph of peak shift vs strain for 1046 cm^{-1} (solid square) and 1018 cm^{-1} (solid diamond) peaks as well as the 1022 cm^{-1} peak in the original spectrum (open circle with standard deviation). The arrow indicates the peak shift after the film was torn.

changes due to the Si−O bond length, the Si−O−Si angle, the O−Si−O angle, and the angle through which the silica tetrahedra have rotated.[24] Work is under way to model the deformation in the clay layers through computer simulation to compare with FTIR results.

Since the strains were low and the peak shift showed fairly linear behavior, the mode of deformation is likely to be the same up to failure. Note that the strain axis in Figure 3 refers to the macroscopic strain of the whole sample, not the clay particles. In a particulate composite, the load under tension is transferred from the matrix to the particles via the matrix/particle interface shear stress. A simple model to predict the stress distribution along a discontinuous particle in a matrix in the elastic state is the shear-lag analysis developed by Cox for a single cylindrical reinforcing fiber embedded in a soft cylindrical matrix.[25] Recent finite element studies of polymer/layered silicate nanocomposites in two dimensions have demonstrated that the results for a reinforcing component shaped like a flat disk are qualitatively similar to the shear-lag analysis.[26] For simplicity, we shall use Cox's model in our discussion. From the shear-lag analysis, the axial strain ϵ_f in the fiber is given by

$$\epsilon_f = \epsilon_m\left[1 - \frac{\cosh \beta\left(\frac{L}{2} - x\right)}{\cosh \beta \frac{L}{2}}\right] \qquad (1)$$

for $0 < x < L$ where

$$\beta = \sqrt{\frac{2G_m}{E_f r^2 \ln\left(\frac{R}{r}\right)}}$$

where ϵ_m is the matrix strain, L is the fiber length, E_f is the fiber modulus, G_m is the shear modulus of the matrix, r is the fiber radius, and R is the distance between neighboring fibers. Equation 1 shows that increasing the matrix strain would cause an increase in the level of strain (or stress) in the particle. The Si−O stretching peak in the nylon-6/nanoclay nanocomposite contains contributions from each vibrational moiety in every particle and from the ensemble of particles within the infrared beam. Our experimental data, which indicate that the stress-induced frequency shift (averaged over a group of nanoclay platelets) in the nanoclay increases with matrix strain, are qualitatively consistent with the shear-lag analysis. This shows that there is transfer of load from the matrix to the nanoclay particles.

Furthermore, Cox's model also predicts that at a given matrix strain the particle strain is low at the end of the particle and increases toward a plateau near the center of the particle. The particle strain (or stress) distribution and level depend on at least three important parameters: (a) particle aspect ratio r/L, (b) matrix to particle stiffness ratio G_m/E_f, and (c) degree of strain shielding between neighboring particles. With increasing particle aspect ratio or the matrix to particle stiffness ratio, the breadth of the plateau increases and its value increases up to a maximum value equal to the matrix strain ϵ_m. Because of the relatively small surface area of the nanoclay platelets (~1000 Å in diameter)[1] compared to the ~5 mm diameter spot size of the infrared beam (the smallest attainable size being about 1 mm in diameter), it is beyond our experimental capability to monitor the strain distribution across each individual platelet. Nevertheless, we can perform a simple analysis. Though the elastic modulus of montmorillonite clay has not been measured, the modulus of a similar material, mica, has been determined to be 180 GPa in the plane of one layer and 70 GPa in the direction perpendicular to this plane.[27] For nylon-6, the maximum modulus has been experimentally determined to be 165 GPa along the chain direction of the α crystal[28] and found to be as low as 0.80 GPa in the amorphous regions.[29] Substituting a particle modulus of 180 GPa,[27] matrix modulus of 0.80 GPa,[29] particle length of 1000 Å,[1] particle radius of 1 nm, and R/r value of 10 into eq 1, the maximum value of particle strain ϵ_f is calculated to be only 91% of the matrix strain. The result from this calculation seems to indicate that the load transfer from the matrix to the clay particles is not very effective, possibly due to the low aspect ratio of the clay particles or the strain shielding effect. Further studies can clarify this issue, test the validity of the theoretical models at the nanolength scale, and evaluate the set of parameters needed to optimize the mechanical properties of the nylon/nanoclay nanocomposite.

Conclusions. This is the first time that stress-induced peak shifts in the Si−O stretching vibration of montmorillonite clay in a polymer nanocomposite system have been observed by FTIR. This offers a way to monitor how the clay particles deform relative to the polymer matrix. Insights into mechanical deformation behavior at the nanoscale level can then be obtained from such experiments. This technique to study micromechanics of nanoclay reinforced polymer matrices is superior to X-ray scattering in observing the deformation process and can be extended to other spectroscopic techniques such as Raman spectroscopy.

Acknowledgment. The authors thank Dr. J. S. Shelley and Dr. H. Nonaka for providing the nylon-6 materials and information regarding the samples as well as Professor R. E. Cohen for discussion and the use of the spin-casting equipment. This research was sponsored by the DURINT on Microstructure, Processing and Mechanical Performance of Polymer Nanocomposites, Air Force Contract No. F49620-01-1-0047.

Note Added after ASAP Posting. This communication was released ASAP on 3/19/2003. More details were added to the Acknowledgment. The revised version was posted on 3/24/2003.

References and Notes

(1) Kojima, Y.; Usuki, A.; Kawasumi, M.; Okada, A.; Fukushima, Y.; Kurauchi, T.; Kamigaito, O. *J. Mater. Res.* **1993**, *8*, 1185−1189.
(2) Kojima, Y.; Usuki, A.; Kawasumi, M.; Okada, A.; Kurachi, T.; Kamigaito, O. *J. Appl. Polym. Sci.* **1993**, *49*, 1259−1264.
(3) Vaia, R. A.; Price, G.; Ruth, P. N.; Nguyen, H. T.; Lichtenhan, J. *J. Appl. Clay Sci.* **1999**, *15*, 67−92.
(4) Lincoln, D. M.; Vaia, R. A.; Wang, Z.-G.; Hsiao, B. S. *Polymer* **2001**, *42*, 1621−1631.
(5) Wu, H.-D.; Tseng, C.-R.; Chang, F.-C. *Macromolecules* **2001**, *34*, 2992−2999.
(6) Mathias, L. J.; Davis, R. D.; Jarrett, W. L. *Macromolecules* **1999**, *32*, 7958−7960.
(7) Cho, J. W.; Paul, D. R. *Polymer* **2001**, *42*, 1083−1094.
(8) Masenelli-Varlot, K.; Reynaud, E.; Vigier, G.; Varlet, J. *J. Polym. Sci., Part B: Polym. Phys.* **2002**, *40*, 272−283.
(9) Kim, G.-M.; Lee, D.-H.; Hoffmann, B.; Kressler, J.; Stoppelmann, G. *Polymer* **2001**, *42*, 1095−1100.
(10) Sakurada, I.; Kaji, K. *J. Polym. Sci., Part C* **1970**, *31*, 57−76.
(11) Zhurkov, S. N.; Vettegren, V. I.; Novak, I. I.; Kashincheva, K. N. *Dokl. Akad. Nauk USSR* **1967**, *176*, 623−626.
(12) Zhurkov, S. N.; Vettegren, V. I.; Korsukov, V. E.; Novak, I. I. *Fiz. Tverd. Tela* **1969**, *11*, 290−295.
(13) Vettegren, V. I.; Novak, I. I.; Friedland, K. J. *Int. J. Fract.* **1975**, *11*, 789−801.
(14) Tashiro, K.; Minami, S.; Wu, G.; Kobayashi, M. *J. Polym. Sci., Part B: Polym. Phys.* **1992**, *30*, 1143−1155 and references therein.
(15) Robinson, I. M.; Young, R. J.; Galiotis, C.; Batchelder, D. N. *J. Mater. Sci.* **1987**, *22*, 3642−3646.
(16) Boogh, L. C. N.; Meier, R. J.; Kausch, H. H.; Kip, B. J. *J. Polym. Sci., Part B: Polym. Phys.* **1992**, *30*, 325−333.
(17) Young, R. J.; Andrews, M. C. *Mater. Sci. Eng.* **1994**, *A184*, 197−205.
(18) Andrews, M. C.; Bannister, D. J.; Young, R. J. *J. Mater. Sci.* **1996**, *31*, 3893−3913.
(19) Cooper, C. A.; Young, R. J. *J. Raman Spectrosc.* **1999**, *30*, 929−938.
(20) Usuki, A.; Kojima, Y.; Kawasumi, M.; Okada, A.; Fukushima, Y.; Kurauchi, T.; Kamigaito, O. *J. Mater. Res.* **1993**, *8*, 1179−1184.
(21) Rotter, G.; Ishida, H. *J. Polym. Sci., Part B: Polym. Phys.* **1992**, *30*, 489−495 and references therein.
(22) Farmer, V. C.; Russell, J. D. *Spectrochim. Acta* **1964**, *20*, 1149−1173.
(23) Wu, Q.; Liu, X.; Berglund, L. A. *Polymer* **2002**, *43*, 2445−2449.
(24) Yan, L.; Roth, C. B.; Low, P. F. *Langmuir* **1996**, *12*, 4421−4429.
(25) Cox, H. L. *Br. J. Appl. Phys.* **1952**, *3*, 72−79.
(26) Sheng, N. Masters Thesis, Massachusetts Institute of Technology, 2002.
(27) McNeil, L. E.; Grimsditch, M. *J. Phys.: Condens. Matter* **1993**, *5*, 1681−1690.
(28) Sakurada, I.; Kaji, K. *J. Polym. Sci., Part C* **1970**, *31*, 57−76.
(29) Prevorsek, D. C.; Harget, P. J.; Sharma, R. K.; Reimschuessel, A. C. *J. Macromol. Sci., Phys.* **1973**, *B8*, 127−156.

MA0259057